

Lifshitz transitions and quasiparticle de-renormalization in YbRh_2Si_2

H. R. Naren,^{1,*} S. Friedemann,² G. Zwicknagl,³ C. Krellner,^{1,†} C. Geibel,¹ F. Steglich,¹ and S. Wirth¹

¹*Max Planck Institute for Chemical Physics of Solids, Nöthnitzer Str. 40, 01187 Dresden, Germany*

²*Cavendish Laboratory, University of Cambridge, Cambridge CB3 0HE, UK*

³*Institut für Mathematische Physik, TU Braunschweig, Mendelssohnstr. 3, 38106 Braunschweig, Germany*

(Dated: September 15, 2018)

We study the effect of magnetic fields up to 15 T on the heavy fermion state of YbRh_2Si_2 via Hall effect and magnetoresistance measurements down to 50 mK. Our data show anomalies at three different characteristic fields. We compare our data to renormalized band structure calculations through which we identify Lifshitz transitions associated with the heavy fermion bands. The Hall measurements indicate that the de-renormalization of the quasiparticles, *i.e.* the destruction of the local Kondo singlets, occurs smoothly while the Lifshitz transitions occur within rather confined regions of the magnetic field.

I. INTRODUCTION

YbRh_2Si_2 is a well-studied heavy fermion compound¹ which has an antiferromagnetic (AFM) ground state below $T_N = 70$ mK. The corresponding AFM transition can be suppressed to zero temperature by the application of a small magnetic field $B_N = 60$ mT (660 mT) perpendicular (parallel) to the crystallographic c direction of the tetragonal lattice structure. Right at B_N indications for the existence of a quantum critical point (QCP) have been observed². At fields higher than B_N , the system resides in a heavy Fermi liquid state below a crossover temperature T_{FL} . There is an extended considerably large regime of non-Fermi liquid (NFL) behavior fanning out above the QCP in the $B - T$ phase space. This QCP is believed to be unconventional, in that it involves the breakup of Kondo singlets at fields below a certain field $B^{\text{Hall}}(T)$ which coincides with the QCP at zero temperature, and can be traced up to much higher temperatures³.

The $J = 7/2$ multiplet state of the Yb^{3+} ions is split into four Kramers doublets by the crystalline electric field (CEF) within the tetragonal structure of YbRh_2Si_2 . Kondo scattering over the entire $J = 7/2$ multiplet gives a Kondo temperature estimate of $T_K^{\text{high}} \approx 80$ K from the minimum observed in thermopower measurements⁴ (in our notation of a high Kondo temperature, T_K^{high} , and a lower one, T_K^{low} , we rely on Ref.⁵). However, since the separation between the ground state doublet and the first excited CEF state is large⁶ (~ 200 K), the ground state doublet dominates the Kondo scattering at low temperatures. The single-ion Kondo temperature of the ground state doublet, $T_K^{\text{low}} \equiv T_K$, has been estimated from entropy considerations via specific heat measurements⁷ to $T_K \approx 25$. Moreover, thermopower measurements⁴ on magnetically diluted $\text{Lu}_{1-x}\text{Yb}_x\text{Rh}_2\text{Si}_2$ yielded $T_K \approx 29$ K for YbRh_2Si_2 . In general, there is a third energy scale, T_{coh} , which denotes the temperature below which Kondo-lattice coherence sets in and hybridized heavy fermion bands form. However, at least in the case of YbRh_2Si_2 , Scanning Tunneling Microscopy (STM) measurements⁸

provided evidence that the Kondo-lattice coherence develops once the $4f$ electrons have sufficiently condensed into the CEF ground state, *i.e.* that $T_K \approx T_{coh}$. Therefore, we will use T_K for this scale henceforth. One focus here is to study the fate of the heavy quasiparticles in the Kondo systems YbRh_2Si_2 in high magnetic fields.

Applying a magnetic field to a heavy fermion system can cause several effects: One is similar to increasing the temperature in that the single-ion Kondo effect is increasingly weakened. Another is Zeeman splitting which may become significant by inducing Lifshitz transitions (LTs), *i.e.* a band may get spin-split beyond the Fermi energy E_F , or the Fermi surface topology may change drastically. Zeeman splitting is practically insignificant in normal metals since the relevant energy scale E_F is of the order of few eV which corresponds to magnetic fields of about 10^4 T. In heavy fermion metals, however, this scale is greatly reduced due to the hybridization of conduction and localized f electrons via the Kondo effect.

A further effect can be a metamagnetic transition which many heavy fermion compounds undergo at a characteristic magnetic field \hat{B} applied along the easy direction of magnetization. A few examples are CeRu_2Si_2 ($\hat{B} \approx 7.8$ T, Ref.^{9,10}), CeTiGe (12 T, Ref.¹¹), UPt_3 (20 T, Ref.¹²) and CeCu_6 (4 T, Ref.¹³). The former three compounds show a sharp jump in the field-dependent magnetization at \hat{B} whereas the latter one only exhibits a kink at \hat{B} . Moreover, in CeTiGe there are indications¹¹ for a first order phase transition at \hat{B} . The metamagnetic transition in CeRu_2Si_2 , which has extensively been investigated with respect to this issue, was initially attributed to a destruction of the Kondo effect resulting in the increase of magnetization¹⁰. The field scale $\hat{B} = 7.8$ T was believed to correspond to the Kondo energy scale of ~ 20 K in this system beyond which the f electrons were thought to become localized. However, the metamagnetic transition was later argued¹⁴ to result from a LT, a conclusion based on transport measurements, model calculations and a re-interpretation of de Haas-van Alphen (dHvA) results.

A corresponding scale $\hat{B} \approx 10$ T for YbRh_2Si_2 along its

crystallographic ab plane (which is the easy plane of magnetization) was estimated from a kink in magnetization⁷. Moreover, the quantities depending on the density of states (DOS), like the magnetic susceptibility, the Sommerfeld coefficient of the electronic specific heat γ , the A -coefficient of the resistivity ϱ (within Fermi liquid theory $\varrho = \varrho_0 + AT^2$ where ϱ_0 is the residual resistivity) and the linear magnetostriction coefficient all decrease in a pronounced fashion around this field. The decrease in DOS, *cf.* Fig. 1(c), was interpreted as a destruction of the heavy fermion state¹⁵ and $\hat{B} \approx 10$ T could experimentally be related to the Kondo energy scale via $k_B T_K \approx g \mu_B \hat{B}$ (k_B and μ_B are the Boltzmann constant and the Bohr magneton, respectively; $g \sim 3.5$ is the g factor¹⁶). Another reasoning for the association of \hat{B} and T_K was based on the identical pressure dependence of the two quantities⁷.

A dHvA study of YbRh_2Si_2 revealed¹⁷ a gradual reduction of the dHvA frequency across \hat{B} . This was interpreted in terms of a LT, *i.e.*, at \hat{B} one of the spin-split components of a heavy band is shifted beyond the Fermi level. Calculations based on static¹⁸ and dynamic mean field theory¹⁹ endorsed the LT scenario to be responsible for the anomaly at \hat{B} . Another argument against an alternative explanation, namely the destruction of the heavy fermion state, would be the sizeable value of γ of around 100 mJ/mol K² even beyond 10 T. This value is much larger than the one reported²⁰ for the local moment analogue LuRh_2Si_2 (6.5 mJ/mol K²).

In this work, we report on a high-resolution study of magnetotransport (Hall effect and magnetoresistance) on high-quality single crystals of YbRh_2Si_2 and concentrate on high magnetic fields (up to 15 T, in contrast to earlier reports^{3,21} which focused on the QCP at small fields) in order to shed light on these transitions. These measurements are facilitated by renormalized band structure calculations to support our assertions (for the ease of discussion we start off with presenting these results first). While topological changes of the Fermi surface may not necessarily reflect a significant change of the DOS, they can create new open or closed orbits. Thus, transport measurements can be a very sensitive tool to study such changes.

II. RENORMALIZED BAND CALCULATIONS WITH APPLIED MAGNETIC FIELD

The renormalized band calculations for YbRh_2Si_2 have also been extended to study the magnetic field evolution of the DOS²². The influence of the magnetic field is accounted for by field-dependent values for the centers-of-gravity $\tilde{\epsilon}_{fm}(B)$ and effective widths $\hat{\Delta}_{fm}(B)$ of the renormalized f -bands which are obtained from fits to the field-dependent quasiparticle DOS of the single-impurity Anderson model^{23–26}. The latter are calculated by means of the numerical renormalization group (NRG). The iso-

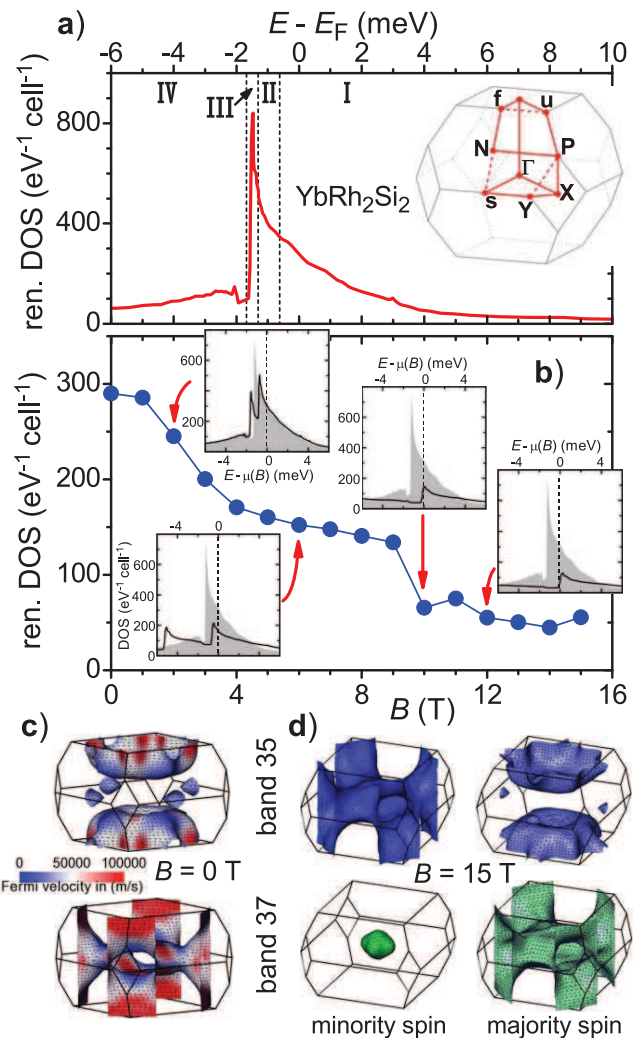


FIG. 1. Renormalized band structure calculations on YbRh_2Si_2 . a) Energies close to E_F displaying the van Hove singularity and the division into four regions (marked I to IV) separated by Lifshitz transitions (marked by dashed lines). Inset illustrates the directions. b) Variation of the renormalized DOS with magnetic field. Insets: DOS(E) at different magnetic fields clearly showing a Zeeman splitting of the van Hove singularity (for comparison, the zero-field DOS is shown in grey in the background, same scales are used for all insets). c) Calculated Fermi surfaces for the two main bands 35 and 37. Colors indicate the Fermi velocity. d) Fermi surfaces at 15 T for the same two bands and for majority and minority spin direction.

ergy surfaces in zero field can be correlated to the Fermi surfaces within a magnetic field in terms of the position of the Fermi energy with respect to the van Hove singularity of the minority spin DOS. These surfaces are expected to be topologically similar without and with field even though the height of the van Hove singularity itself decreases with field, see insets to Fig. 1(b).

Figure 1(a) displays the zero-field DOS from which, in particular, the partially developed hybridization gap and

a van Hove singularity can be recognized. These features are found below E_F as expected for a hole (Yb-based) system. Four regions can be identified within the investigated energy range within which the isoenergy surfaces mainly keep their topology and which are labeled I–IV in Fig. 1(a)²⁷. The transitions between these regions are marked by LTs, dashed lines in Fig. 1(a).

With increasing field, the calculated DOS exhibits a progressive reduction, with a marked jump at 10 T (see Fig. 1(b)). These calculations indicated that the quasiparticle de-renormalization, *i.e.* the field-induced suppression of the Kondo effect, takes over rather smoothly and hence, by itself cannot create the anomaly at 10 T²². The field evolution of the DOS as depicted in the insets of Fig. 1(b) involves the Zeeman splitting of the zero-field DOS. With increasing magnetic field the majority spin van Hove singularity sweeps rapidly away from the Fermi level while the minority spin van Hove singularity crosses E_F at around 10 T (see insets). In addition, the peak height of the van Hove singularity reduces with increasing field owing to the de-renormalization of the quasiparticles. Clearly, it takes the renormalized band calculation including both the above-mentioned effects as well as the quasiparticle interactions to reproduce a field evolution of the DOS which conforms to the variation of the Sommerfeld coefficient and thermopower²⁷.

Fermi surfaces have been calculated for the two bands predominantly contributing to the DOS. These two bands, band 35 and 37, give rise to the so-called ‘pillow’ (upper picture in Fig. 1(c)) and ‘jungle-gym’ (lower picture), respectively. The color code in Fig. 1(c) indicates the Fermi velocity. Upon shifting the majority spin DOS(B) to lower energies by increasing the magnetic field the topology of its Fermi surfaces remains largely unchanged, right column in Fig. 1(d), since E_F stays within region I of the DOS. In contrast, the minority spin Fermi surfaces strongly change when the minority spin DOS(B) moves up in energy and its corresponding E_F travels through regions I–IV²⁷. Consequently, LTs are encountered in the minority spin DOS(B). The prominent one within band 35 is the formation of a single, connected surface upon crossing from region II to III, Fig. 1(d). The isoenergy surface of band 37 undergoes a ‘neck-forming’ LT in the crystallographic direction $\Gamma \rightarrow X$ between regions I and II (for directions see inset to Fig. 1(a)), followed by a ‘neck-disrupting’ LT at an angle between $\Gamma \rightarrow X$ and $\Gamma \rightarrow s$ and a ‘pocket-disappearing’ LT of the pocket along $X \rightarrow P \rightarrow u$ upon entering region IV.

As is obvious from this insets to Fig. 1(b), the dominant peak of the minority spin van Hove singularity is shifted beyond E_F at around 10 T. Since the width of this peak is supposed²⁸ to be the same as T_K , this again indicates that the magnetic field scale of 10 T is indeed the equivalent of T_K . From the magnitude of the shift of the minority van Hove singularity, we can assign magnetic field values to the transitions between the different regions: The corresponding LTs are calculated to take place at $B_1 = 2.5 \pm 1$ T (region I to II), at $B_2 = 9 \pm 1$ T (region

II to III), and from region III to IV at $B_3 = 11 \pm 1$ T.

Depending on the extent of contribution of a specific band to the DOS, the corresponding LTs are expected to cause changes in the DOS(B), Fig. 1(b). A kink is seen at around B_1 , a drop at B_2 and a small maximum at B_3 . However, the kink at B_1 is, to some extent, already visible in the DOS(B) just due to the de-renormalization of the quasiparticles²². Thus, the LT at B_1 seems to have a very minor effect on the DOS. This can be understood²² from the fact that the dominant contribution to the zero-field DOS stems from the ‘pillow’ Fermi surface while it is the ‘jungle-gym’ one that undergoes a LT at B_1 . The comparatively large jump at B_2 is likely caused by both, the ‘pillow’ and the ‘jungle-gym’, sheets being subject to LTs. In contrast, the faint feature at B_3 is solely due to the LT of the erstwhile ‘jungle-gym’ sheet whose contribution appears to be more significant at high fields, perhaps due to a reduced contribution from the erstwhile ‘pillow’ sheet. We note that the features at B_1 and B_3 were not obvious in magnetization or heat capacity measurements⁷, but could be resolved in thermopower^{27,29}. In our magnetotransport measurements, we clearly observe all these features as well as indications related to the de-renormalization of quasiparticles.

III. EXPERIMENTAL

We performed *simultaneous* isothermal magnetoresistance (MR) and Hall effect measurements down to $T \geq 50$ mK and in magnetic fields up to $B \leq 15$ T. To facilitate direct comparison, current j and B were applied perpendicular to the crystallographic c direction for both, MR ($j \parallel B$) and Hall measurements. Consequently, the Hall voltage V_H was to be measured along the c direction. Since YbRh₂Si₂ cleaves perpendicular to the c axis, we used two different crystals (from the same batch, also same batch as in Ref.³⁰) with optimized geometries for the respective measurements. Note that these are among the highest-quality crystals of YbRh₂Si₂ (residual resistivity $\sim 0.5 \cdot 10^{-8} \Omega\text{m}$). For optimized sensitivity the sample for Hall measurements was thinned down to 70 μm , and the signals were consecutively amplified by low-temperature transformers, low-noise amplifiers and lock-in amplifiers for both types of measurements. The actual Hall voltage was taken as the antisymmetric component of the measured Hall voltage under field reversal³¹.

IV. MAGNETORESISTANCE

Figure 2 exhibits the field-dependent resistivity $\varrho_{xx}(B)$, the magnetoresistance $\text{MR} = \frac{\varrho_{xx}(B) - \varrho_{xx}(B=0)}{\varrho_{xx}(B=0)}$ and the field derivative of MR. The MR is positive at lowest temperatures, as expected for the coherent state. At 50 mK and 15 T, the resistivity enhancement over the

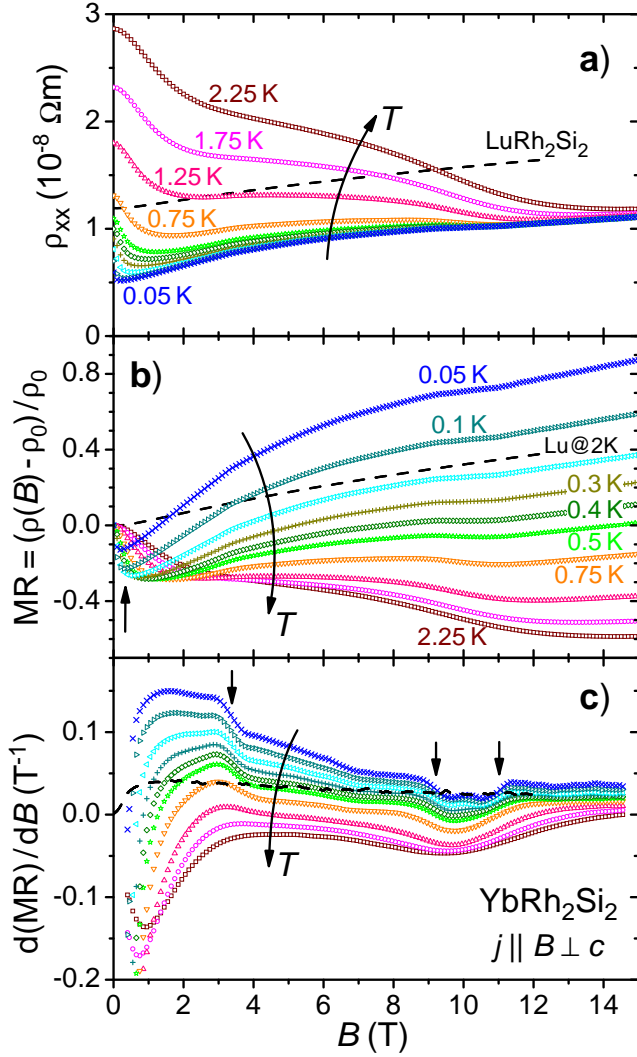


FIG. 2. a) Field dependence of resistivity $\rho_{xx}(B)$, b) of magnetoresistance and c) of its field derivative as functions of magnetic field. All panels exhibit results at the same selected temperatures, $0.05 \text{ K} \leq T \leq 2.25 \text{ K}$, and the same color code. Black dashed lines: results of the nonmagnetic reference compound LuRh_2Si_2 at $T = 2 \text{ K}$.

zero-field value is close to 90%. At very low fields, a step-like transition is visible (marked by an upward arrow in Fig. 2(b)) at lowest temperatures which gets smeared out quickly as temperature increases. This has been reported to be a signature of the Fermi surface reconstruction related to the unconventional QCP in this compound²¹. With increasing T , ρ_{xx} at low fields increases due to progressive inelastic scattering of conduction electrons. The negative MR at higher T is then a result of the magnetic-field suppression of the spin-flip scattering.

At fields above 3 T, a small kink in the MR is observed that is clearly reflected as a step in its derivative, marked by an arrow in Fig. 2(c). A feature at this field scale has not been observed in previous measurements even though it should be expected from the kink seen in

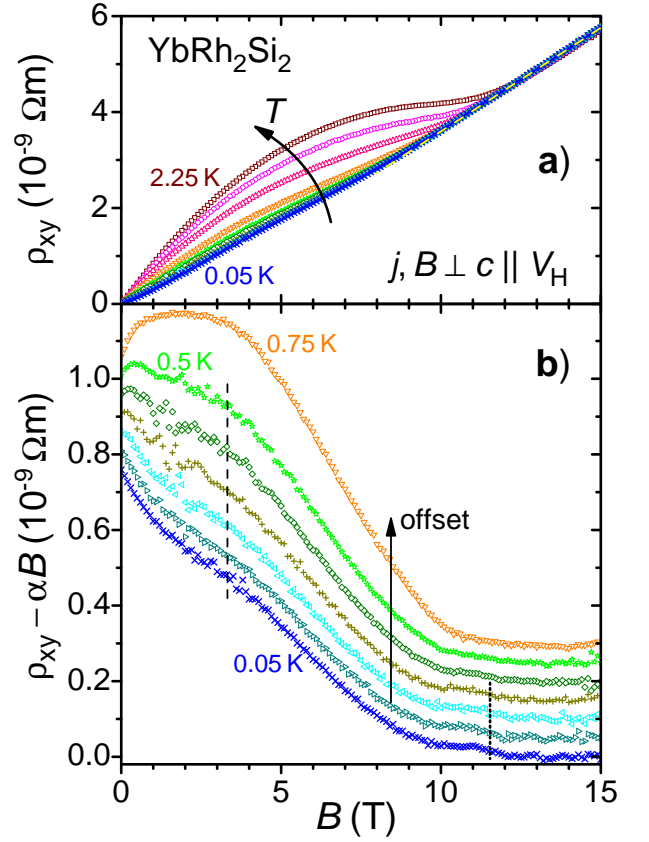


FIG. 3. Results of isothermal Hall effect measurements (same temperatures and symbols as in Fig. 2). a) Field dependence of Hall resistivity $\rho_{xy}(B)$. The dashed line indicates the linear high-field slope. b) Same low- T $\rho_{xy}(B)$ data as in a) but with the linear high-field slope subtracted, $\rho_{xy}(B) - \alpha \cdot B$. For further clarity, curves (except at 50 mK) are offset by $0.5 \cdot 10^{-10} \Omega\text{m}$. Dashed/dotted lines are guides to the eye.

the $\text{DOS}(B)$ ²². The anomaly observed at 10 T in Ref.⁷ appears as a double kink in our MR data, again marked by arrows in Fig. 2(c). The two kinks are roughly at 9 T and 11 T and are most sharply visible at lowest $T = 50 \text{ mK}$. Although these kinks get smeared out at higher temperatures their positions in field remain roughly the same. Thus, we indeed observe signatures of all the three predicted LTs in our MR data.

At fields beyond 12 T, *i.e.* beyond the high field anomaly, the MR appears to become linear in field, at least at low temperature. In fact, the linear regions in the low-temperature $\rho_{xx}(B)$ -curves nicely overlap implying a temperature independent high-field state. This point of view is further supported by results obtained on the non-magnetic reference compound LuRh_2Si_2 which exhibits a featureless MR throughout the measured field range (up to 12 T) with a slope very similar to the high-field MR in YbRh_2Si_2 . Such an increase of the MR is in line with the existence of open orbits in the Fermi surface of YbRh_2Si_2 at higher fields, Fig. 1(d).

V. HALL MEASUREMENTS

We now focus on the results of our Hall measurements presented in Fig. 3. It has been shown that in YbRh_2Si_2 at temperatures below 1 K the anomalous contribution to the Hall effect data is less than a few percent³². In both models considered in Ref.³², the anomalous Hall contribution is proportional to the magnetic susceptibility χ . Since $\chi(B)$ goes down for increasing fields B , the anomalous contribution to the Hall effect is expected to continue to be insignificant even at the high fields we have measured in. In contrast, at higher temperatures the anomalous Hall contribution becomes dominant. For example, the Hall resistivity ρ_{xy} at $T = 2.25$ K in Fig. 3(a) appears to largely resemble the magnetization curve measured earlier⁷. We note here that, unfortunately, a comparison to Hall measurements on the nonmagnetic reference compound LuRh_2Si_2 was defied by the extremely small size of the LuRh_2Si_2 single crystals.

The most intriguing result is the collapse of all measured curves $\rho_{xy}(T, B)$ at high fields into a single, linear-in-field curve, *i.e.* $\rho_{xy}(T, B)$ appears to be independent of temperature, see dashed line in Fig. 3(a). The field value beyond which this collapse occurs increases with temperature. Since the anomalous Hall contribution is small at lowest temperature (see above), the temperature independence of $\rho_{xy}(T, B \gtrsim 12$ T) at high fields also implies that the anomalous contribution becomes very small for *all* measured temperatures at high fields. In turn, this implies that the system at sufficiently high fields behaves largely like an ordinary paramagnetic metal, even though it is polarized. This view is corroborated by the fact that the field-derived energy scale at which these ordinary metallic properties occur corresponds to the energy scale T_K^{low} relevant at the low temperatures investigated in the present study.

At low temperature (below 0.5 K), the isothermal $\rho_{xy}(T, B)$ curves appear almost linear in B . However, there are subtle changes of slope that become apparent if a (large) linear “background” is subtracted. In Fig. 3(b), we plot $\rho_{xy}(T, B) - \alpha \cdot B$, where the constant α corresponds to the T -independent high-field slope of $\approx 4.7 \cdot 10^{-11} \Omega\text{m}/\text{T}$. For clarity, an increasing offset (by $0.5 \cdot 10^{-10} \Omega\text{m}$) was added to the $\rho_{xy}(T, B)$ -curves above 50 mK. There is a clear inflection point at around 3 T (marked by a vertical dashed line) which corresponds to the inflection seen in the $\text{DOS}(B)$, Fig. 1(b). This feature develops into a maximum at higher temperatures, likely as a result of the additional anomalous contribution to $\rho_{xy}(T, B)$. Moreover, $\rho_{xy}(T, B)$ at lower temperatures exhibits a step-like decrease at around 11 T (dotted line cutting through low- T curves only) which gets smeared out at higher temperatures. This decrease, which seems to appear at constant fields at different temperatures, is likely related to the third LT at B_3 .

To gain insight into the evolution of the Fermi surface we now consider the Hall coefficient $R_H = \partial \rho_{xy}(T, B) / \partial B|_T$. The most prominent feature in Fig.

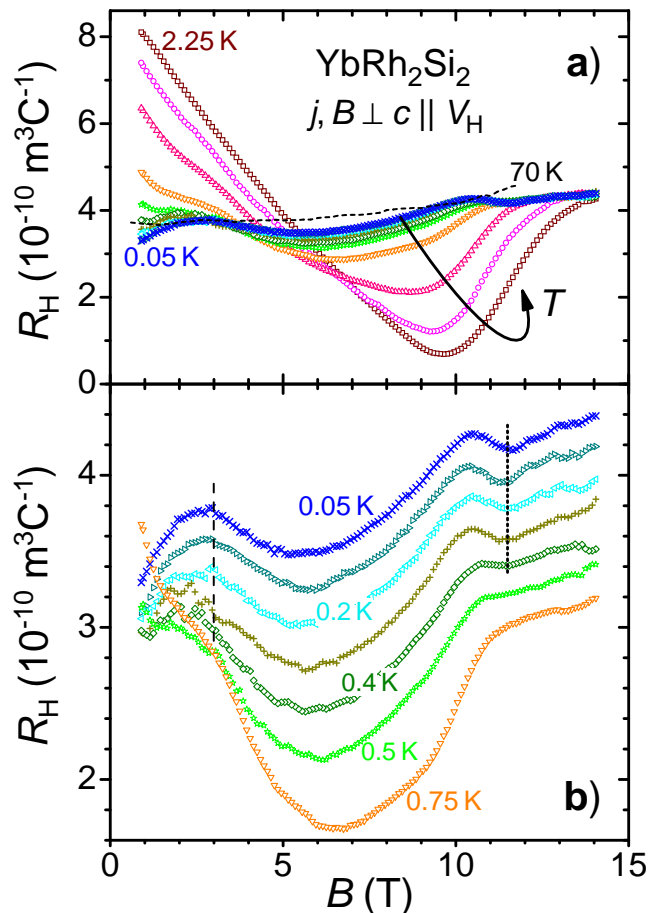


FIG. 4. a) Hall coefficient R_H (same temperatures and symbols as in Figs. 2 and 3). The dashed line represents data at 70 K. b) Magnified view of the low- T data. Curves at increasing T are offset *downward* by $0.2 \cdot 10^{-10} \text{ m}^3\text{C}^{-1}$ for clarity. At low T , the normal Hall contribution dominates.

4(a) is the minimum in R_H at fields of roughly 9 T. This minimum strongly develops with increasing temperature (above 0.5 K) and shifts its position towards higher field indicating that it is *not* related to the DOS³³. Rather, it appears to be caused by fluctuations evolving upon leaving the Fermi liquid regime with increasing T . Such behavior is in line with a model³⁴ which describes the temperature evolution of R_H by skew scattering related to the on-site Kondo effect, rather than coherent effects. This temperature evolution of R_H (as measured at 0.5 T) is presented in Fig. 5 and resembles the one obtained³ for $B||c$. It confirms our conjecture above that R_H is dominated by the normal contribution, *i.e.* it is related to the DOS, only at lowest temperatures or at high fields $B \gtrsim 12$ T. Inspecting the low- T curves of R_H , Fig. 4(b), an anomalous Hall contribution appears to set in at $T = 0.75$ K as signaled by the dent observed around 9 T. We therefore concentrate on the lowest measured temperatures in the following, Fig. 4(b).

At $T \leq 0.2$ K, a maximum in R_H is observed around 3 T (dashed line in Fig. 4(b)). In all likelihood this feature

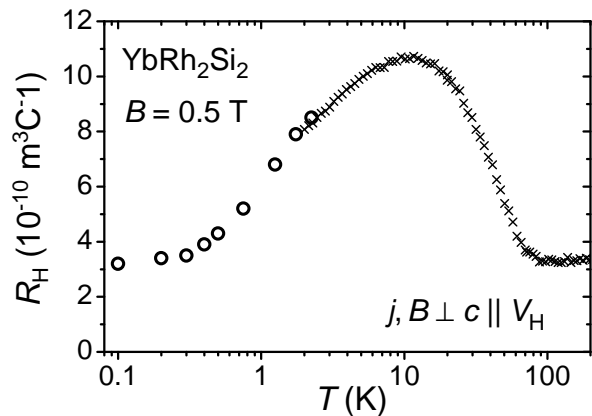


FIG. 5. Temperature dependence of the Hall coefficient R_H at 0.5 T. Data marked by crosses (\times) were obtained on the *same* sample but using a Magnetic Properties Measurement System (MPMS).

is related to the LT at B_1 , *i.e.* the inflection in $\text{DOS}(B)$ and above-mentioned neck formation along the $\Gamma \rightarrow X$ direction. Interestingly, among the three transitions, the one at B_1 appears to have the most pronounced effect on R_H resulting in the corresponding maximum.

Upon increasing field there is a clear minimum in R_H visible at around 11.5 T and for $T \leq 0.4$ K, without apparent shift for different temperatures (as indicated by the dotted line). One may therefore speculate that this feature is related to the LT at B_3 . At this field, there is a maximum in $\text{DOS}(B)$, see Fig. 1(b), along with severe changes in the topology of the Fermi surfaces at these fields. The combination of these two effects may account for the somewhat higher field values at which the transitions are observed in R_H compared to the calculations. On the other hand, there is no clear feature seen in R_H in the field range around 9 T. As noted above (*cf.* Fig. 1) there are two major bands at E_F , both undergoing LTs. We speculate that the transitions in these two bands compensate each other such that the net change in R_H is weak. We note here that thermopower measurements²⁷ on a sample of the same batch and for identical orientation also showed a maximum-minimum feature at fields around 11 T, but an additional, second maximum at around 9.5 T. While this nicely corroborates our Hall data the occurrence of an additional maximum also hints at the fact that electrical and thermal transport measurements could be differently sensitive to these phenomena.

At low T an increasing background is visible in R_H upon increasing B , best seen in Fig. 4(b). This background is even obvious in R_H measured at 70 K (obtained on the same sample but in a different measurement sys-

tem limiting the absolute quantitative comparison). Such an increase suggests a reduction in the number of charge carriers (in the simplest model, $R_H = -1/e n_{\text{eff}}$ where n_{eff} is the effective charge carrier concentration and e is the charge of an electron). This may be taken as another indication for the progressive de-renormalization of quasiparticles at high magnetic fields, *i.e.* of the on-site Kondo interaction. In other words, the f -electrons seem to be gradually driven out of the Fermi volume with increasing magnetic field. It nicely confirms the evolution of the Kondo effect with decreasing temperature as discussed in the introduction: the fact that the increase of R_H with field is still seen at 70 K, *i.e.* below T_K^{high} but well above T_K , clearly points towards the single-ion nature of this effect.

Our measurements indicate a rather smooth delocalization-localization transition at high fields. These observations are in line with the already mentioned fact⁷ that the Sommerfeld coefficient remains as large as ~ 100 mJ/molK² beyond 10 T and is much larger than the value of LuRh₂Si₂. In contrast, there is clear evidence from renormalized bandstructure calculations that the observed features at the different fields B_1 , B_2 and B_3 could be due to Lifshitz transitions which appear more abrupt in field.

A generic low-field Lifshitz transition was predicted³⁵ via DMFT calculations on the Kondo lattice model. Indeed, we do observe such a transition in YbRh₂Si₂ in our measurements. In addition, Lifshitz transitions have been predicted to occur at high fields in heavy fermion systems^{18,19}, at the scale given³⁵ by T_K . However, we find two closely spaced Lifshitz transition near 10 T. This could be due to a slight difference in the coupling of the two bands to the magnetic field.

VI. CONCLUSION

We have shown several Lifshitz transitions to occur in YbRh₂Si₂, by severe changes of the Fermi surface topology of the dominating bands vis-à-vis the shifting of the Zeeman-split Kondo resonance through E_F . While these transitions occur rather abruptly, the de-renormalization of the quasiparticles takes place comparatively smoothly. This phenomenology could be generic among heavy fermion compounds, and magnetotransport seems to be a useful tool in addressing such issues.

We thank H. Pfau and M. Brando for insightful discussions. This work is partly supported by the German Research Foundation through DFG Forschergruppe 960.

* present address: Department of Condensed Matter Physics, Weizmann Institute of Science, 76100 Rehovot,

Israel
† present address: Goethe-University Frankfurt, Institute of

- Physics, 60438 Frankfurt/Main, Germany
- ¹ O. Trovarelli, C. Geibel, S. Mederle, C. Langhammer, F. M. Grosche, P. Gegenwart, M. Lang, G. Sparn and F. Steglich, *Phys. Rev. Lett.* **85**, 626 (2000).
 - ² P. Gegenwart, J. Custers, C. Geibel, K. Neumaier, T. Tayama, K. Tenya, O. Trovarelli and F. Steglich, *Phys. Rev. Lett.* **89**, 056402 (2002).
 - ³ S. Paschen, T. Lühmann, S. Wirth, P. Gegenwart, O. Trovarelli, C. Geibel, F. Steglich, P. Coleman and Q. Si, *Nature* **432**, 881 (2004).
 - ⁴ U. Köhler, N. Oeschler, F. Steglich, S. Maquilon and Z. Fisk, *Phys. Rev. B* **77**, 104412 (2008).
 - ⁵ B. Cornut and B. Coqblin, *Phys. Rev. B* **5**, 4541 (1972).
 - ⁶ O. Stockert, M. M. Koza, J. Ferstl, A. P. Murani, C. Geibel and F. Steglich, *Physica B* **378-380**, 157 (2006).
 - ⁷ P. Gegenwart, Y. Tokiwa, T. Westerkamp, F. Weickert, J. Custers, J. Ferstl, C. Krellner, C. Geibel, P. Kersch, K.-H. Müller and F. Steglich, *New J. Phys.* **8**, 171 (2006).
 - ⁸ S. Ernst, S. Kirchner, C. Krellner, C. Geibel, G. Zwicknagl, F. Steglich and S. Wirth, *Nature* **474**, 362 (2011).
 - ⁹ J. Flouquet, S. Kambe, L. P. Regnault, P. Haen, J. P. Brison, F. Lapierre and P. Lejay, *Physica B* **215**, 77 (1995).
 - ¹⁰ J. Flouquet, P. Haen, S. Raymond, D. Aoki and G. Knebel, *Physica B* **319**, 251 (2002).
 - ¹¹ M. Deppe, S. Lausberg, F. Weickert, M. Brando, Y. Skourski, N. Caroca-Canales, C. Geibel and F. Steglich, *Phys. Rev. B* **85**, 060401 (2012).
 - ¹² K. Sugiyama, M. Nakashima, D. Aoki, K. Kindo, N. Kimura, H. Aoki, T. Komatsubara, S. Uji, Y. Haga, E. Yamamoto, H. Harima and Y. Ōnuki, *Phys. Rev. B* **60**, 9248 (1999).
 - ¹³ T. Sakakibara, T. Goto, Y. Ōnuki and T. Komatsubara, *J. Magn. Magn. Mater.* **70**, 375 (1987).
 - ¹⁴ R. Daou, C. Bergemann and S. R. Julian, *Phys. Rev. Lett.* **96**, 114709 (2006).
 - ¹⁵ G. Knebel, R. Boursier, E. Hassinger, G. Lapertot, P. G. Niklowitz, A. Pourret, B. Salce, J. P. Sanchez, I. Sheikin, P. Bonville, H. Harima and J. Flouquet, *J. Phys. Soc. Jpn.* **75**, 026401 (2006).
 - ¹⁶ U. Schaufuß, V. Kataev, A. A. Zvyagin, B. Büchner, J. Sichelschmidt, J. Wykhoff, C. Krellner, C. Geibel and F. Steglich, *Phys. Rev. Lett.* **102**, 076405 (2009).
 - ¹⁷ P. M. C. Rourke, A. McCollam, G. Lapertot, G. Knebel, J. Flouquet and S. R. Julian, *Phys. Rev. Lett.* **101**, 237205 (2008).
 - ¹⁸ S. V. Kusminskiy, K. S. D. Beach, A. H. Castro Neto, and D. K. Campbell, *Phys. Rev. B* **77**, 094419 (2008).
 - ¹⁹ K. S. D. Beach and F. F. Assaad, *Phys. Rev. B* **77**, 205123 (2008).
 - ²⁰ S. Friedemann, S. Wirth, N. Oeschler, C. Krellner, C. Geibel, F. Steglich, S. MaQuilon, Z. Fisk, S. Paschen and G. Zwicknagl, *Phys. Rev. B* **82**, 035103 (2010).
 - ²¹ S. Friedemann, N. Oeschler, S. Wirth, C. Krellner, C. Geibel, F. Steglich, S. Paschen, S. Kirchner and Q. Si, *Proc. Natl. Acad. Sci. USA* **107**, 14547 (2010).
 - ²² G. Zwicknagl, *J. Phys.: Condens. Matter* **23**, 094215 (2011).
 - ²³ A. C. Hewson, A. Oguri and D. Meyer, *Eur. Phys. J. B* **40**, 177 (2004).
 - ²⁴ A. C. Hewson, J. Bauer and W. Koller, *Phys. Rev. B* **73**, 045117 (2006).
 - ²⁵ J. Bauer and A. C. Hewson, *Phys. Rev. B* **76**, 035119 (2007).
 - ²⁶ R. Peters, T. Pruschke and F. B. Anders, *Phys. Rev. B* **74**, 245114 (2006).
 - ²⁷ H. Pfau, R. Daou, S. Lausberg, H. R. Naren, M. Brando, S. Friedemann, S. Wirth, T. Westerkamp, U. Stockert, P. Gegenwart, C. Krellner, C. Geibel, G. Zwicknagl and F. Steglich, arXiv:1302.6867.
 - ²⁸ T. A. Costi and N. Manini, *J. Low Temp. Phys.* **126**, 835 (2002).
 - ²⁹ A. Pourret, G. Knebel, G. Lapertot, T. D. Matsuda and J. Flouquet, arXiv:1302.7298.
 - ³⁰ N. Oeschler, S. Hartmann, A. P. Pikul, C. Krellner, C. Geibel and F. Steglich, *Physica B* **403**, 1254 (2008).
 - ³¹ S. Nair, S. Wirth, M. Nicklas, J. L. Sarrao, J. D. Thompson, Z. Fisk and F. Steglich, *Phys. Rev. Lett.* **100**, 137003 (2008).
 - ³² S. Paschen, T. Lühmann, S. Wirth, O. Trovarelli, C. Geibel and F. Steglich, *Physica B* **359**, 44 (2005).
 - ³³ A. Fert and P. M. Levy, *Phys. Rev. B* **36**, 1907 (1987).
 - ³⁴ P. Coleman, P. W. Anderson and T. V. Ramakrishnan, *Phys. Rev. Lett.* **55**, 414 (1985).
 - ³⁵ M. Bercx and F. F. Assaad, *Phys. Rev. B* **86**, 075108 (2012).